Geopersia 2022, 12(1): 127-139
DOI: 10.22059/GEOPE.2021.327205.648625

RESEARCH PAPER

Thermochemical analysis of the oil shale from the Middle Jurassic Sargelu Formation, Southwest Iran: A thermo-oxidative approach

Ali Shekarifard *

School of Chemical Engineering, College of Engineering, University of Tehran, Tehran, Iran

Received: 14 July 2021, Revised: 13 November 2021, Accepted: 07 December 2021

Abstract
In this study, thirteen surface samples were selected and investigated to characterize the thermal decomposition process of the oil shale from the Sargelu Formation (Middle Jurassic) in Lorestan province (Southwest Iran). The oil shale samples, for the first time, were studied using Differential Scanning Calorimetry (DSC) and the non-isothermal Thermogravimetric (TG-DTG) analysis with heating rates of 5, 10, and 15 °C/min. Thermo-oxidative decomposition of the Sargelu oil shale was occurred in three steps: (1) the thermo-oxidation of bitumen (according to the heating rate ranging from 210 °C to 401 °C), (2) the thermo-oxidation of the kerogen (between 365 and 560 °C), and (3) finally, the decomposition of calcite mineral (between 541°C and 815 °C). The thermal experiments show that the peak temperatures and reaction region intervals increased to greater temperatures by an increase in the heating rate. The activation energy parameter analyzed through the oil shale thermo-oxidative kinetics was evaluated using the ASTM E-698, Ozawa-Flynn-Wall (OFW) and Kissinger-Akahira-Sunose (KAS) approaches. The mean activation energy calculated during low-temperature thermo-oxidative of the Sargelu oil shale is 127 KJ/mol. Compared to the Early Cretaceous Garau oil shale with the mean activation energy of 183 KJ/mol from the same locality, the Sargelu oil shale has lower activation energy. Eventually, kinetics analysis confirmed the occurrence of kerogen with (very) fast reaction rate in the Sargelu oil shale.

Keywords: Thermo-oxidative decomposition, Sargelu oil shale, Middle Jurassic, Lorestan, Iran.

Introduction

In a highly broad meaning, the oil shale is described as a fine-grained sedimentary rock including an organic matter (OM) that yields economic amounts of oil and combustible gas upon thermochemical destructions. The major component of the OM is kerogen, which is a cross-linked macromolecular matter that is insoluble in solvents at conventional conditions. Another part of the OM in the oil shale is represented by solvent-soluble bitumen. Oil shale widely range in kerogen and bitumen content, chemical compositions, and oil yields. Heat energy and electric power can be generated by the direct thermo-oxidative of the oil shale. In order to produce liquid fuels, gas, and chemicals, thermochemical destruction of oil shale organic matter is used.

Thermogravimetry (TG) is a branch of physical chemistry, materials research, and thermal analysis and is based on the continuous recording of the mass changes of a given sample, as a function of a combination of temperature with time, as well as pressure and gas composition (neutral or oxidizing). In this technique, also named thermo-balance, a given sample (varying from 1 to 100 mg) is located on an arm of a recording microbalance, and both are then located in a furnace. A pre-programmed temperature/time profile, or in the rate-controlled mode is used

* Corresponding author e-mail: ashekary@ut.ac.ir

to control the furnace temperature. The temperature variation is imposed by the pre-programmed value of weight changes imposes for achieving and maintaining the desired weight-change rate.

TG Analysis (TGA) and Differential TG Analysis (DTG) are common tools for investigating thermal behaviors, the characteristics of devolatalization, and the kinetic parameters of solid materials (including oil shale) by accurate measuring of the mass change of the samples, which have been subjected to a temperature program. There are different studies and applications in the investigation of the oil shale from different resources in the world (e.g., KöK & Pamir, 1995, 1998, 2000; Lisboa & Watkinson, 1999; Li & Yue, 2003; KöK et al., 2004; Olivella, 2006; Qing et al., 2006; KöK, 2007; KöK & Iscan, 2007; Qing et al., 2007; Johannes & Zaidentsal, 2008; Zhang et al., 2021). The effects of the flow rate, the purity and nature of gas, the particle size, and the sample amount on the thermal behavior of the oil shale and the reliability of the obtained findings were assessed via TGA (Lisboa & Watkinson, 1999).

Many research studies have shown that the thermogravimetric (TG/DTG) analysis technique under non-isothermal heating conditions is one of the most advanced methods for estimating the thermal behavior of the oil shale. In calculations, the oxidation of the oil shale is defined by the first-order kinetics, in which greater activation energy values are achieved at greater reaction temperatures (Vyazovkin & Wight, 1998; KöK & Pamir, 1995, 2000; KöK et al., 2004; KöK & Iscan, 2007; Vyazovkin et al., 2011; Skala et al., 1987; Warne & Dubrawski, 1989; Finucane et al., 1977; Rajeshwar & DuBow, 1982; Burnham et al., 1983; Williams & Ahmad, 2000; Kök et al., 2001; Johannes & Zaidentsal, 2008; Tiwari & Deo, 2012).

Differential scanning calorimetry (DSC) is a thermoanalytical technique in which the difference in the amount of heat required to increase the temperature of a sample and reference is measured as a function of temperature. In this approach, the variation in the heat content is essential for increasing the temperature of a sample. During the analysis, both the reference and sample are kept at approximately the equal temperature. The temperature program for a DSC method is mainly designed so that a linear increase in sample holder temperature occurs as a function of time. A proper heat capacity is to be adopted for the reference sample across the range of temperatures that need scanning. DSC cannot only provide the temperature at which the transition takes place and the amount of the involved heat, but also significant data about the kinetics or rate of the reaction (KöK & Pamir, 1998, 2003, 2003; KöK, 2007).

The present study is the first one to determine the thermo-oxidative decomposition characteristics of the Sargelu oil shale, which is highly essential for the assessment of the potential of utilizing the oil shale of Iran in the future, along with comparing the Sargelu oil shale with the deposits of the Garau oil shale. Furthermore, the Sargelu Formation is considered as one of the main effective source rocks in southwest Iran thus the kinetics calculation is needed for the thermal modeling of this Formation where it has been buried deeply.

Material and Methods

Oil shale samples

The oil shale samples belong to the upper part of the Sargelu Formation (Middle Jurassic) from Lorestan province in the southwest of Iran (Shekarifard et al., 2014; Rasouli et al., 2015). The Lorestan province is placed in the southwest of Iran in the Zagros Mountain Range. At the study area, two oil shale intervals are recognized; one from the upper part of the Sargelu Formation and second one from the lower part of the Garau Formation (Early Cretaceous) (Figure 1). At the investigated locality, the Sargelu Formation is unconformably overlain by the Upper Jurassic Najmeh Formation.

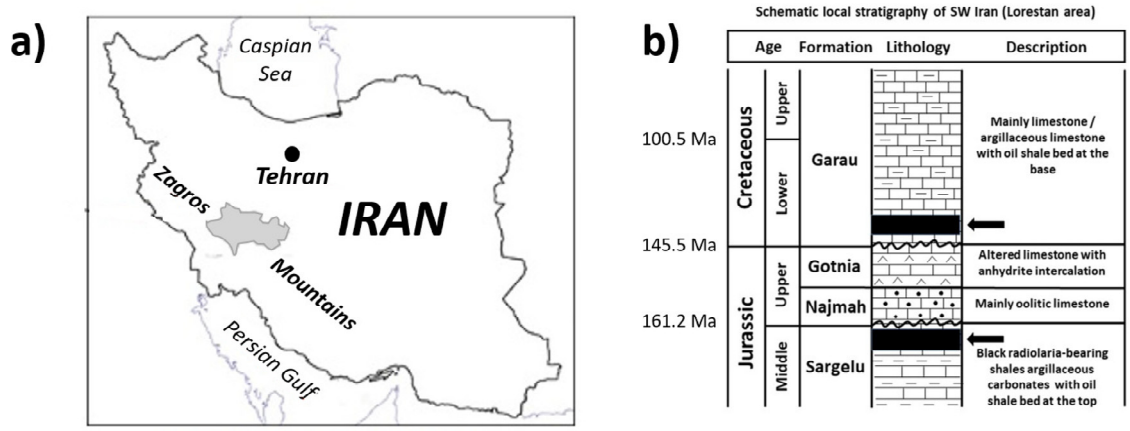

Figure 1. (a) Lorestan province in SW Iran, (b) local stratigraphy of the study area with oil shale intervals (arrows)

The Najmeh Formation consists of oolitic limestones with some scattered crystals of dolomite, alternating with limestone layers and thin anhydride layers. It is sometimes disconformably overlain by the Gotnia Formation. These Upper Jurassic rock units record a steady upward-shallowing change from relatively deeper water sedimentary conditions to lagoonal environments and also supratidal to fully subaerial conditions. The Garau Formation begins with a 2-3 meters thin-bedded limestone which is covered by black oil shale layer. This Formation is primarily comprised of argillaceous limestone with intercalations of shale containing *Radiolarids* and *Posidonia* shells. Figure 1 shows the local stratigraphy of the study area.

In this study, 13 oil shale samples were systematically selected from two localities of the study area from the Sargelu Formation. The identical aliquots of the oil shale samples were collected from each sample and were then crushed, mixed, and homogenized (particle size <60 mesh with the ASTM D 2013-72 standard) to obtain a representative oil shale sample from each locality (samples GHx and SHx). The representative samples of the Sargelu oil shale from two different outcrop sections. This standard would help to eliminate the effect of temperature distributions while considering bulk and homogeneous samples.

Experimental methods

Bulk geochemical characterization of the oil shale was performed using a Rock-Eval VI pyrolysis apparatus (Behar et al., 2001). The standard notations used include S_1 peak (free hydrocarbons) and S_2 peak (pyrolysate of kerogen plus heavy hydrocarbon (HC) species resins plus asphaltenes) in mg HC per g of rock; S_3 peak (generated CO_2) in mg CO_2 / g rock; Tmax is expressed in °C; total organic carbon (TOC) the content in weight percentage, hydrogen index ($HI = S_2 \times 100 / TOC$) in mg HC per g of TOC, oxygen index ($OI = S_3 \times 100 / TOC$) in mg CO_2 per g of TOC, and production index ($PI = S_1 / (S_1 + S_2)$). Table 1 presents the results of the Rock-Eval pyrolysis on the representative samples from the Sargelu oil shale.

The distribution of obtained products when the oil shale sample is heated under particular conditions can be measured using proximate analysis. According to ASTM D-121, the products are separated into four groups in the proximate analysis (1) moisture, (2) volatile matter, including vapors and gases driven off throughout pyrolysis, (3) fixed carbon, the non-volatile fraction of the oil shale, and (4) ash, as the inorganic residue remaining after thermo-oxidative. This test also includes the determination and estimation of the oil shale heating value. The proximate analysis results of the Sargelu oil shale samples are summarized in Table 2.

The hydrogen and carbon content in the material can be determined using the ultimate analysis is described in ASTM D-3176. It is also used to determine the gaseous products of its

complete thermo-oxidative, as well as the sulfur, nitrogen, and ash in the material as a whole, and estimate oxygen by differences. The Ultimate analysis results of the Sargelu oil shale samples are summarized in Table 3.

An X-Ray diffractometer (XRD) was used for minerals identification using two diffractometers. Furthermore, a Axios X-ray Fluorescence (XRF) spectrometer was employed to measure the amount of significant element oxides and some trace elements. The findings of the XRD (a) and XRF (b) analyses are presented in Table 4.

A TG analyzer was performed to assess the thermal behavior of the Sargelu oil shale. The samples were subjected to three constant 5, 10, 15 ˚C/min heating rates from 20 ˚C up to 900 ˚C and the experiments were performed twice. This series of non-isothermal measurements helped to have a proper calculation of kinetic parameters (Vyazovkin et al., 2011). Air atmosphere with a 50 ml/min approximate flow rate was performed (thermo-oxidative) as the purge gas through the thermochemical process. The in-situ computer measured the mass change as a function of temperature and provided the electronic differentiation of mass loss (differential TG, DTG) in each temperature.

Table 1. Rock-Eval results of the representative samples from the Sargelu oil shale

Sample ID	TOC	S_1	S_2	S_3	T_{max}	HI	OI	PI
GHx	20.5	2.0	92.9	2.2	432	453	11	0.02
SHx	17.9	2.7	92.7	0.7	438	518	4	0.03
Mean	**19.2**	**2.3**	**92.8**	**1.45**	**435**	**485**	**6**	**0.02**

Table 2. Proximate analysis of the representative samples from the Sargelu oil shale (as received basis)

Sample ID	Total Moisture (wt%)	Ash (wt%)	Volatile Matter (wt%)	Fixed Carbon (wt%)	Total Sulfur (wt%)	LHV (kcal/kg)	HHV (kcal/kg)
GHx	0.69	52.67	30.66	15.98	3.79	1841	1927
SHx	0.58	56.98	33.79	8.65	3.61	1698	1778
Mean	**0.63**	**59.50**	**32.22**	**12.27**	**3.7**	**1769**	**1852**

LHV: Low heating value (the products of thermo-oxidative contain the water vapor and that the heat in the water vapor is not recovered)

HHV: High heating value (the water of thermo-oxidative is entirely condensed and that the heat contained in the water vapor is recovered)

Table 3. Ultimate analysis of the representative samples from the Sargelu oil shale.

Sample ID	C (%)	H (%)	N (%)	S (%)	O (%)
GHx	25.89	1.48	0.51	2.41	17.04
SHx	23.85	1.53	0.46	2.64	14.54
Mean	**24.87**	**1.55**	**0.48**	**2.52**	**15.79**

Table 4. XRD (a) and XRF (b) results of the representative samples from the Sargelu oil shale

(a)

Sample ID	Quartz (wt%)	Feldspar Group (wt%)	Calcite (wt%)	Dolomite (wt%)	Pyrite (wt%)
GHx	6	Traces	94	Traces	Traces
SHx	5	Traces	95	Traces	Traces

(b)

Sample ID	Al_2O_3 (%)	CaO (%)	Fe_2O_3 (%)	K_2O (%)	MgO (%)	MnO (%)	Na_2O (%)	P_2O_5 (%)	SO_3 (%)	SiO_2 (%)	TiO_2 (%)
GHx	5.4	52.3	3.0	1.5	1.0	<0.1	0.1	0.4	13.4	19.1	0.4
SHx	2.7	59.2	3.2	0.8	0.6	<0.1	0.2	1.0	14.9	13.9	0.1
Mean	**4.1**	**55.8**	**3.1**	**1.2**	**0.8**	**<0.1**	**0.1**	**0.7**	**4.2**	**16.5**	**0.3**

Ozawa-Flynn-Wall (OFW) and Kissinger-Akahira-Sunose (KAS) methods were applied to estimate and analyze the activation energy and TG-DTG data. In this study, oil shale thermo-oxidative kinetics by the DSC technique was carried out in the air atmosphere up to 600 ˚C at three constant 5, 10, and 15 ˚C/min heating rates. The ASTM E-698 kinetics approach was utilized for analyzing the DSC data.

Results and Discussion

General characterization

Rock-Eval VI analysis

Total organic carbon (TOC) content is considered a fundamental parameter for the evaluation of oil shale resources. According to the results obtained, the TOC content of the representative Sargelu oil shale from the study locality varies from 17.9 to 20.5 wt%, with a mean value of 19.2 wt%. Based on the Rock-Eval VI pyrolysis data, the mean hydrogen index (HI) value of the representative samples is 485 mg HC/g TOC. The remaining potential (S_2 parameter) for the samples is reaching up to 92.9 mg HC/g rock. These critical Rock-Eval parameters reflect excellent potential for oil generation. The T_{max} value (average: 435°C) and production indices (0.02 - 0.03) show that the Sargelu and Garau oil shale have a maturity just at the start of the oil-window. The HI and OI values confirm the presence of predominately Type I-II kerogen.

Proximate analysis

The heat value of the Sargelu oil shale is more than 1698 kcal/kg with a mean value of 1810 Kcal/kg. The higher ash content usually leads to a lower heating value. The moisture amount of the oil shale in the proximate analysis involves inherent and external moisture. The moisture of the oil shale samples is extremely low (on average: 0.59 wt%), in comparison to the oil shale used in the industry with a moisture content of slightly over 10% (Plamus et al., 2011; Konist et al., 2013). According to Shekarifard et al., 2021, the Garau oil shale shows lower content of total moisture (0.39 wt%). The mean ash content of the Sargelu oil shale is 57.4 wt%, which is slightly more than that of the Garau oil shale (Ash = 52.99 wt%).

Ultimate analysis

The sulfur content of the samples is between 2.41 and 2.64 % (Table 3). The Sargelu oil shale samples demonstrate higher content of sulfur (Mean sulfur = 2.52%) in comparison to the Garau oil shale (Mean sulfur = 1.81%) (Shekarifard et al., 2021). The oxygen content is high, offering the transference of oil shale oxygen into gaseous or liquid products throughout the pyrolysis process. This represents that the high temperature retorting of the oil shale is unfavorable due to the extensive generation of CO_2 gas.

XRF and XRD analysis

To identify the chemical composition and the mineralogy of the representative Sargelu oil shales, XRF and XRD analyses were used, respectively. The CaO content is extremely high in comparison to the very low MgO amount, indicating the occurrence of high amounts of calcite. However, the low percentage of Mg shows that there might be dolomite in these samples even in negligible amounts. In agreement with the XRF data, the XRD trial results also imply the existence of calcite, maximum peak, as the main inorganic mineral in the oil shale (Figure 2).

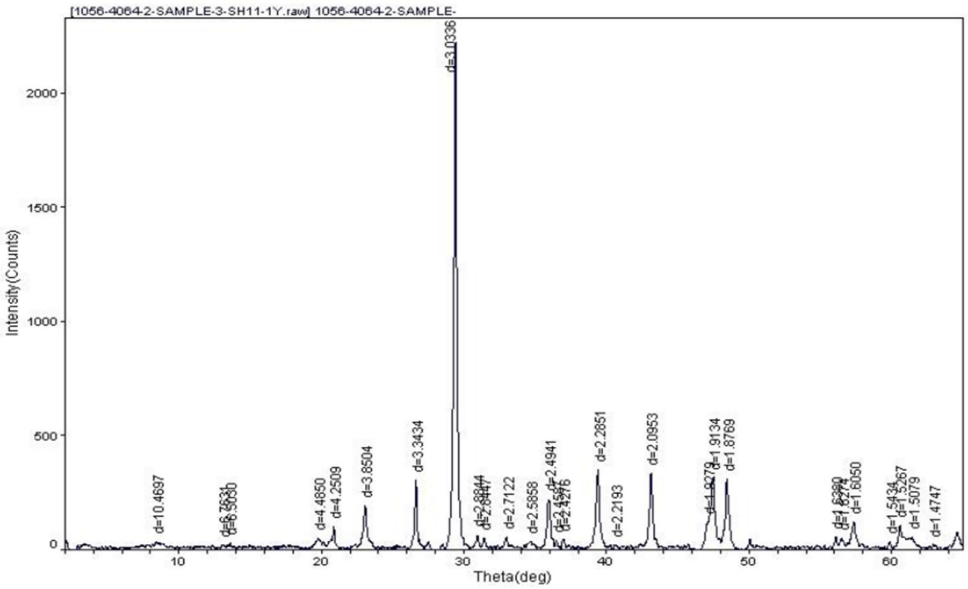

Figure 2. XRD pattern of the representative sample SHx from the Sargelu oil shale

Quartz mineral appears as a minor phase in the investigated oil shales. The representative samples demonstrate that the clay minerals might exist in the content of samples due to the existence of aluminum and iron minerals. The low amount of sodium and potassium in the samples represents that the feldspar (clay minerals) amount in the studied samples is negligible. Generally, the mineralogy of the Sargelu and the Garau oil shale is similar (Shekarifard et al., 2021).

Thermo-oxidative decomposition of the oil shale

DSC analysis

As a complicated process, oil shale thermo-oxidative includes a group of parallel reactions. In general, depending on oil shale properties, oil shale thermo-oxidative is a two-step process, including the thermo-oxidative of bitumen (the light organic part in the oil shale) and the thermo-oxidative of kerogen (the heavy organic part in the oil shale). Table 5 provides the results of the representative samples from the Sargelu oil shale in Lorestan. Two peaks are observed during OM decomposition.

In the thermo-oxidative of the Sargelu oil shale samples, according to the observations, below ~130 ˚C oil shale loses the moisture thus the H_2O components in the crystalline structure are decomposed using DSC. The organic content, mainly comprising kerogen and bitumen, is decomposed between 210-560 ˚C (depending on the heating rate). According to the obtained data in Table 5, the first reaction interval corresponds to the thermo-oxidation of volatile organic compounds (depending on the heating rate between 210 and 401 ˚C), and the second reaction interval shows the thermo-oxidation of the heavier part of kerogen and the fixed carbon (365-560 ˚C). Furthermore, an increase in the heating rate leads to further release of energy since the loss of volatile particles decreases prior to thermo-oxidative owing to de-volatilization (Table 5). Simultaneously, the ignition temperature is reached earlier by the increased heating rate, leading to a decrease in devolatilization (loss of the OM) time. Moreover, the peak temperatures and reaction region intervals increased to greater temperatures by an increase in the heating rate. Figures 3 and 4 illustrate DSC curves for the representative oil shale samples.

Table 5. DSC results of the representative samples from the Sargelu oil shale

Sample ID	Heating Rate (ºC/min.)	Reaction I interval (ºC)	Reaction II interval (Peak Temp.) (ºC)*	Heat of Reaction (J/gr)	Heat Flow Rate (mW)
GHx	5	228-368	368-496 (440)	1603	45,62
	10	235-391	391-505 (462)	2062	108,2
	15	246-401	401-529 (477)	2080	154,3
SHx	5	210-365	365-531 (425)	1339	37,88
	10	217-384	384-542 (447)	1338	75,83
	15	234-397	397-560 (458)	1489	117,9

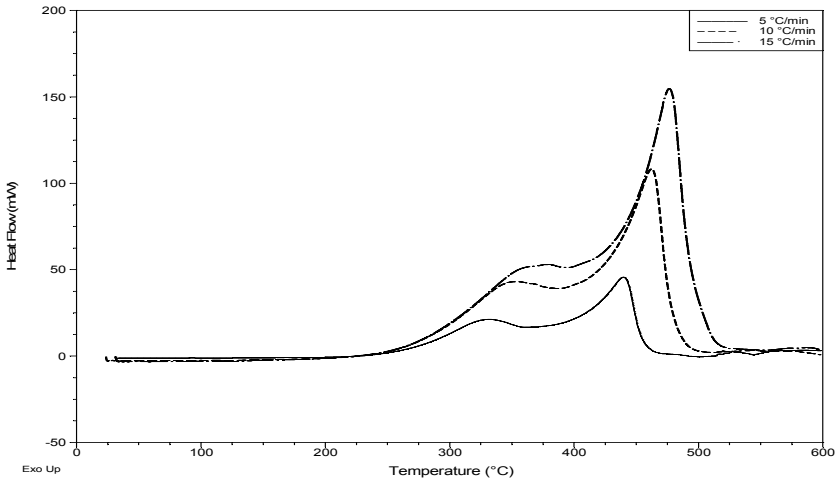

Figure 3. DSC curves of the representative sample GHx

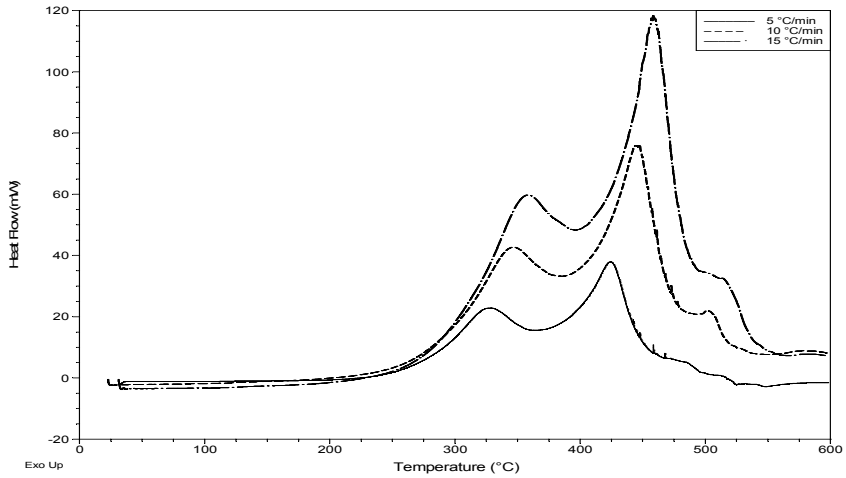

Figure 4. DSC curves of the representative sample SHx

TG-DTG analysis

Based on data in Figures 5 and 6, the TG-DTG profiles (mass-loss and its derivative) for the Sargelu oil shale indicate that the decomposition occurs in two reaction steps, low-temperature (first peak) and high-temperature (second peak) reaction intervals, similar to the Garau oil shale (Shekarifard et al., 2021).

The low-temperature and high-temperature reaction intervals are due to the OM decomposition and the breaking down of the calcite, respectively. The mass loss is less than 2 wt% in the samples subjected to any heating rate before 235 ˚C. This phenomenon is mainly

related to moisture and interlayer water release and probably, the volatilization of free hydrocarbons. Table 6 provides the mass loss and the temperature interval of two main reactions for the representative samples from the Sargelu oil shale in each heating rate.

The first reaction interval of mass loss with 22.3-25.47 wt% loss (mean= 23.76 wt%) is in the range of 235-591 ˚C. In the samples, DTG curves demonstrate one clear peak, showing the overall straightforward single-stage dominant OM decomposition reaction. By increasing the heating rate, the mass loss fluctuates and the first temperature peak shifts to higher temperatures while the reaction transpires in a wider temperature interval, especially with the higher latter temperature.

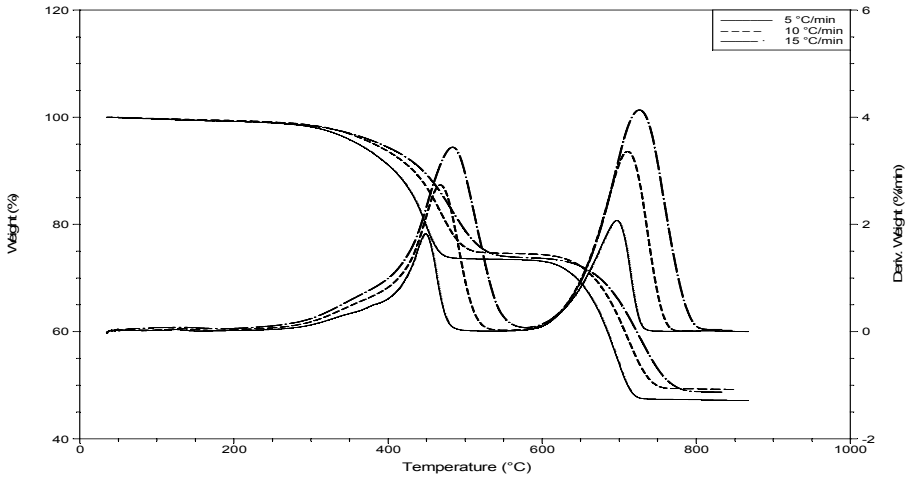

Figure 5. TG-DTG curves of the representative sample GHx

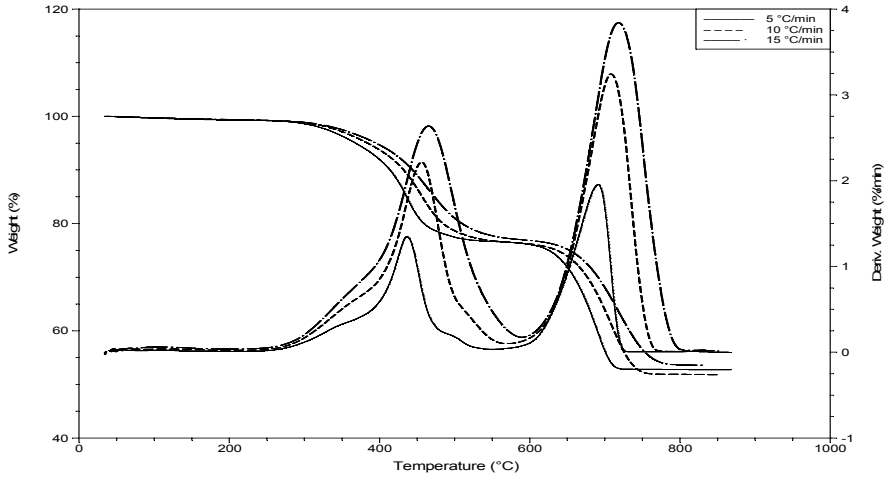

Figure 6. TG-DTG curves of the representative sample SHx

Table 6. TG-DTG results of the representative samples from the Sargelu oil shale

Sample ID	Heating Rate (ºC/min.)	Reaction I interval (Peak Temp.) (ºC)	Mass Loss I (wt%)	Reaction II interval (Peak Temp.) (ºC)	Mass Loss II (wt%)
GHx	5	246-542 (448)	25,47	542-752 (697)	26,11
	10	255-560 (468)	24,48	560-776 (710)	25,24
	15	259-579 (484)	25,06	579-815 (727)	25,06
SHx	5	235-541 (436)	22,51	541-745 (691)	23,91
	10	248-574 (455)	22,74	574-782 (707)	24,61
	15	246-591 (465)	22,30	591-806 (719)	23,33

This phenomenon can be justified by the theory describing the thermal decomposition mechanism of kerogen, which involves a series of parallel non-competitive reactions with different activation energy levels (Behar et al., 2008; Burnham & Happe, 1994; Williams, 1985).

The second reaction interval of mass changes is observed in the range of 541-815 °C with 23.33-26.11 wt% loss (mean= 24.71 wt%). Due to the dominance of calcite mineral (> 94 wt%), the second detected mass loss is due to calcite decomposition. Similar to the first reaction interval, increasing the heating rate leads to a higher reaction temperature peak and response of reaction in a wider temperature interval. The reactants have less time to decompose when the system is subjected to a higher heating rate, causing the reaction in a wider range.

The TG-DTG experiments show the increased peak temperatures and reaction region intervals by increasing heating rate. Despite the similar results for the total mass loss for different heating rates throughout the combustion of the oil shale, the mass loss throughout low-temperature combustion is slightly greater at lower heating rates, likely since the combustion requirements are better at lower heating rates (5 °C/min.)

DSC and TG-DTG kinetics analysis

The oil shale thermo-oxidative kinetics by the DSC technique was carried out in the air atmosphere up to 600 °C at three different heating rates. The ASTM kinetics approach was adopted for analyzing the DSC data (KöK & Pamir, 1998; KöK, 2007).

The non-isothermal kinetics study of the oil shale thermo-oxidative process is complex in the field of the oil shale since there have been several complicated compounds and their consecutive and parallel reactions. According to Brown et al., 2000, in the kinetics project of the International Confederation of Thermal Analysis and Calorimetry (ICTAC), a group of non-isothermal calculations conducted at several heating rates is essential for the precise measurement of kinetics parameters requires (Kissinger, 1957; Ozawa, 1965; Flynn & Wall, 1966). One of the main objects achieved by performing the TG-DTG records is the solid-state decomposition kinetics parameters, especially the activation energy. Therefore, several mathematical approaches are adopted for calculating the relevant data (Sbirrazzuoli et al., 2009; Sbirrazzuoli, 2007).

ASTM kinetics (DSC)

The measurement of overall kinetics factors is covered in ASTM E-698 for exothermic reactions and reactions characterized via the general rate law and the Arrhenius equation. An exact determination of reaction peak temperatures as a function of linear programmed heating rates is required for determining kinetics parameters by peak temperatures. Based on this approach, exothermic peaks caused by increasing the sample temperature in linear heating rates are reported accordingly. The trial-and-error method is applied and the slope in the following equation is used to measure the activation energy:

ASTM-I:

$$E = -2.19 \times R \times [d\log 10\beta / d(1/T)] \quad (1)$$

ASTM-II:

$$E = R \times [d(\ln(\beta / Tp2)] / [d(1 / Tp)] \quad (2)$$

Where; E = activation energy in J/mol, R = ideal gas constant = 8.314 Jmol-1K-1, T =peak temperature in K (Kelvin = °C + 273), β= heating rate in °C/min.

ICTAC kinetics (TG-DTG)

KAS (Kissinger-Akahira-Sunose) Method (E: kJ/mol)

The KAS method was also applied as the isoconversional strategy in which a certain degree of conversion and a narrow temperature range are employed associated with such conversion degree for analyzing the TG-DTG data of the oil shale samples (Table 8). The relationship is as follows:

$$\ln (\beta /T2) = \ln (AR/E\, g(\alpha)) - E/RT \quad (3)$$

Where; α: amount of sample undergoing the reaction; T_p: peak temperature (K); T_o: onset temperature (K); A: pre-exponential parameter (sec^{-1}); R: gas constant; E: activation energy ($kJmol^{-1}$); β is the heating rate ($^oCmin^{-1}$).

OFW (Ozawa-Flynn-Wall) Method (E: kJ/mol)

For the OFW method, different TG-DTG curves were simultaneously utilized for the measurement of the activation energy values of biomass samples. Higher heating rates led to moving the TG-DTG curves to greater temperature levels. For similar conversion amounts, the equation is presented as follows (Table 9). In the following equation, the slope of the plot log (β) vs. 1/T at given conversion levels is used to obtain activation energy.

$$[d (\log \beta) / d (1/T)] = 0.4565 (E / R) \quad (4)$$

Where; E = activation energy in J/mol, R = ideal gas constant = 8.314 Jmol-1K-1, T = temperature in K (Kelvin = ^oC + 273) corresponding to the measured heating rate at same conversion, β= heating rate in ^oC/min.

The above-mentioned kinetics models were utilized to determine the activation energy values of the Sargelu oil shale samples. According to the ASTM kinetic approaches (DSC), interestingly the activation energy of the Sargelu oil shale samples ranges from 121-129 and 121-129 kJ/mol, respectively, based on two different approaches, the same range (Table 7).

In the KAS method, the mean value of the activation energy of the Sargelu oil shale samples range of the conversion level (α) of 0.1-0.9 varied from 130 to 119 kJ/mol and from 237 to 234 kJ/mol for the low-temperature (first) and high-temperature (second) reaction regions, respectively.

Table 7. ASTM Kinetics of the representative samples from the Sargelu oil shale

Sample ID	ASTM -I Activation Energy, kJ/mol	ASTM -II Activation Energy, kJ/mol
GHx	121	121
SHx	129	129

Table 8. KAS Kinetics of the representative samples from the Sargelu oil shale

Sample ID	α	0.1	0.2	0.3	0.4	0.5	0.6	0.7	0.8	0.9	$E_{ave.}$
GHx (I)	E	199	123	111	115	118	115	108	99	87	**119**
GHx (II)		306	276	262	250	239	226	211	194	173	**237**
SHx (I)	E	166	142	138	143	141	130	116	103	95	**130**
SHx (II)		299	275	260	248	236	223	208	190	168	**234**

Table 9. OFW Kinetics of the representative samples from the Sargelu oil shale

Sample ID	α	0.1	0.2	0.3	0.4	0.5	0.6	0.7	0.8	0.9	$E_{ave.}$
GHx (I)	E	199	127	116	120	123	121	114	105	94	**124**
GHx (II)		305	277	264	253	243	230	216	201	180	**241**
SHx (I)	E	166	145	142	147	145	135	122	109	103	**135**
SHx (II)		299	276	262	251	240	227	213	196	176	**238**

The average activation energy values were 124.5 and 235.5 kJ/mol for the first and second reaction regions, respectively. A general trend was detected, representing the lower activation energy of the oil shale samples in the first reaction zone in comparison to the second reaction zone (Table 8).

In the OFW method, the mean value of the activation energy of Sargelu oil shale samples varied from 124 to 135 kJ/mol and from 238 to 241 kJ/mol for the first and second reaction regions in the range of the conversion level (α) of 0.1-0.9, respectively. Moreover, the average activation energy values were 129.5 and 239.5 kJ/mol for the first and second reaction regions, respectively. A general trend was detected, representing lower activation energy of the oil shale samples in the first reaction zone was in comparison to the second reaction zone (Table 9). Compared to the sample SHx, sample GHx with higher content of total sulfur shows lower activation energy. This behavior is observed for many petroleum source rocks that contain high-sulfur kerogen Type IIS kerogen (Hunt, 1996).

Activation energy (E_{ave}) comparison of the Sargelu and Garau oil shale

Based on the calculations, the average activation energy value for the first reaction region (OM decomposition) of the Sargelu oil shale was 127 kJ/mol. According to our previous work on the Garau oil shale and the average activation energy calculated (183 KJ/mol) (Shekarifard et al., 2021), the Sargelu oil shale had lower activation energy. This value of activation energy is extremely low and corresponds to the Type IIS kerogen with a fast reaction rate (Hunt, 1996). Although additional data needs to be added, but the lower activation energy of the Sargelu oil shale is probably attributed to a higher amount of sulfur incorporated into kerogen (Table 4). The C-S bonds are known to have lower bond energies compared to C-C bonds. Some studies reported that kerogens with more sulfur in their structures (S/C ratio > 0.04) have lower activation energies and decompose to low-maturity oils at lower temperatures (Lewan, 1989; Hunt, 1996).

Summary and Conclusion

Despite the similar results for the total mass loss for different heating rates throughout the thermo-oxidative of the Sargelu oil shale, the experiments showed increased reaction region periods and peak temperatures, by increasing the heating rate. Furthermore, according to the results, the reaction intervals are dependent on the heating rate throughout the combustion process.

The apparent activation energy by OFW and KAS methods continuously changed by the conversion rate during the low-temperature thermo-oxidative of the Sargelu oil shale. The kinetics parameters of the calculated oil shale using the OFW method were slightly larger than those of the calculated oil shale by the KAS approach. The average activation energies measured of OFW and KAS approaches were 129.5 and 124.5 kJ/mol, respectively.

Acknowledgments

Authors would like to express their appreciation to the exploration directorate of National Iranian Oil Company (NIOC) for their financial support (Grant no: 89233). Also, the kind cooperation of Prof. Mustafa V. Kök from Middle East Technical University (Ankara, Turkey), and Turkish Petroleum Corporation (TPAO) in the thermal and Kinetics analysis is gratefully acknowledged.

References

Behar, F., Beaumont, V. Penteado, H.D.B., 2001. Rock-Eval 6 technology: performances and

developments. Oil & Gas Science and Technology, 56: 111-134.
Behar, F., Lorant, F., & Lewan, M., 2008. Role of NSO compounds during primary cracking of a Type II kerogen and a Type III lignite. Organic Geochemistry, 39: 1-22.
Brown, M. E., Maciejewski, M., Vyazovkin, S., Nomen, R., Sempere, J., Burnham, A. K., Opfermann, J., Strey, R., Anderson, H. L., Kemmler, A., Keuleers, R., Janssens, J., Desseyn, H. O., Li, C.-R., Tang, T. B., Roduit, B., Malek, J., Mitsuhashi, T., 2000. Computational aspects of kinetic analysis. Thermochimica Acta, 355: 125-143.
Burnham, A. K., Happe, J. A., 1994. On the mechanism of kerogen pyrolysis. Fuel 63: 1353-1356.
Burnham, A. K., Huss, B. E., Singleton, M.F., 1983. Pyrolysis kinetics for Green River oil shale from the saline zone, M. F. Fuel, 62: 1199-1204.
Finucane, D., George, J., Harrist, H., 1977. Perturbation analysis of second-order effects in kinetics of oil-shale pyrolysis, H. G. Fuel, 56: 65-69.
Flynn, J. H., Wall, L. A., 1966. General treatment of the thermogravimetry of polymers, J Res Nat Bur Stand. 70(6): 487-523.
Hunt, M. H., 1996. Petroleum Geochemistry and Geology. W. H. Freeman and Company, 1-743.
Johannes, I., Zaidentsal, A., 2008. Kinetics of low-temperature retorting of kukersite oil shale. Oil Shale, 25:412-25.
Kissinger, H. E., 1957. Reaction kinetics in differential thermal analysis, Analytical Chemistry, 29(11): 1702-1706.
Kök, M.V., 2007. Heating rate effect on the DSC kinetics of oil shale. J Therm Anal Calorim. 90: 817-21.
Kök M.V., Iscan A.G., 2007. Oil shale kinetics by differential methods. J Therm Anal Calorim. 88: 6, 57-61.
Kök, M. V., Pamir M.R., 1998. ASTM kinetics of oil shale. J Therm Anal Calorim. 53: 567-75.
Kök, M. V., Pamir M.R., 2000. Comparative pyrolysis and combustion kinetics of oil shale. J Anal Appl Pyrol. 55: 185-94
Kök, M. V., Pamir M. R., 2003. Pyrolysis kinetics of oil shale determined by DSC and TG/DTG. Oil Shale, 20: 57-68.
Kök, M. V., Pamir, M. R., 1995. Pyrolysis and combustion studies of fossil fuels by thermal analysis methods, Journal of Analytical and Applied Pyrolysis, 35: 145-156.
Kök, M.V., Pokol, G., Keskin, C., Madarász, J., Bagci, S., 2004. Combustion characteristics of lignite and oil shale samples by thermal analysis techniques. J Therm Anal Calorim. 76: 247-54.
Kök, M. V., Senguler, I., Hufnagel, H., Sonel, N., 2001. Thermal and Geochemical Investigation of Seyitömer Oil Shale, Thermochimica Acta, 371: 111-119.
Konist, A.; Pihu, T.; Neshumayev, D.; Siirde, A., 2013. Oil Shale Pulverized Firing: Boiler Efficiency, Ash Balance and Flue Gas Composition. Oil Shale, 30: 6-18
Lewan M. D., 1989. Hydrous pyrolysis study of oil and tar generation from Monterey Shale containing high sulfur kerogen. Amer. Chem. Soc. Natl. Mtg. Abstr., April 9-14. Dallas.
Lisboa ACL, Watkinson AP., 1999. Operating conditions for oil shale thermogravimetry. Powder Technol. 101: 151-6
Olivella M. A., 2006. de las Heras FXC. Nonisothermal thermogravimetry of Spanish fossil fuels. Oil Shale, 23: 340-55.
Plamus K., Soosaar, S., Ots, A., Neshumayev, D., 2011. Firing Estonian Oil Shale of Higher Quality in CFB Boilers—Environmental and Economic Impact. Oil Shale, 28, 113.
Ozawa, T., 1965. A new method of analyzing thermogravimetric data. Bulletin of the chemical society of Japan, 38(11): 1881-1886.
Qing W, Baizhong S, Xiahua W, Jingru B., Jian S., 2006. Influence of retorting temperature on combustion characteristics and kinetic parameters of oil shale semicoke. Oil Shale, 23: 328-39.
Qing W, Baizhong S, Xiahua W, Jingru B, Jian S., 2007. Study on combustion characteristics of Huadian oil shale and semicoke. Oil Shale, 24:135-45.
Li, S. Y., Yue, C .T., 2003. Study of pyrolysis kinetics of oil shale. Fuel, 82(3): 337-342.
Rasouli, A., Shekarifard, A., Jalali Farahani, F., Kök, M. V., Daryabandeh, M. Rashidi, M., 2015. Occurrence of organic-rich deposits (Middle Jurassic to Lower Cretaceous) from Qalikuh locality, Zagros Basin, South-West of Iran: A possible oil shale resource. International Journal of Coal Geology, 143: 34-42.
Rajeshwar, K., DuBow, J. B., 1982. On the validity of a first-order kinetics scheme for the thermal

decomposition of oil shale kerogen, Thermochimica Acta, 54: 71-85.
Sbirrazzuoli, N., 2007. Is the Friedman method applicable to transformations with temperature dependent reaction heat?. Macromolecular Chemistry and Physics, 208: 1592-1597.
Sbirrazzuoli, N., Vincent, L., Mija, A., Guigo, N., 2009. Integral, differential and advanced isoconversional methods, Chemometrics and Intelligent Laboratory Systems, 96: 219-226.
Shekarifard, A., Rasouli, A., Daryabandeh, M., Rashidi, M., 2021. Thermochemical investigation of the oil shale from the Early Cretaceous Garau Formation, Lorestan, SW Iran: Preliminary TGA-FTIR results. Geopersia, 11(2): 289-297.
Shekarifard, A., Jalali Farahani, F., Rashidi, M., Daryabandeh, M., Bagheri, R., Verşan KöK, M., Bjorøy, M., 2014. New data from the oil shale of Iran. the 32th National and 1th International Geosciences Congress, Geological Survey of Iran, Tehran, Ahvaz, 27-28.
Skala, D., Kopsch, H., Sokić, M., Neumann, H.-J., Jovanović, J., 1987. Thermogravi-metrically and differential scanning calorimetrically derived kinetics of oil shale pyrolysis. Fuel, 66: 1185-1191.
Tiwari, P., Deo, M., 2012. Detailed kinetic analysis of oil shale pyrolysis TGA data. AIChE, 58(2): 505-515.
Vyazovkin, S., Wight, C. A., 1998. Isothermal and non-isothermal kinetics of thermally stimulated reactions of solids. International Reviews in Physical Chemistry, 17(3): 407-433.
Vyazovkin, S., Burnham, A. K., Criado, J. M., Pérez-Maqueda, L. A., Popescu, C., Sbirrazzuoli, N., 2011. ICTAC kinetics committee recommendations for performing kinetic computations on thermal analysis data. Thermochimica Acta, 520: 1-19.
Warne, S. S. J., Dubrawski, J. V., 1989. Applications of DTA and DSC to coal and oil shale evaluation. Journal of Thermal Analysis, 35: 219-242.
Williams, P. F. V., 1985. Petroleum geochemistry of the Kimmeridge Clay of onshore Southern and Eastern England. Fuel, 64: 540-545.
Williams, P. T., Ahmad, N., 2000. Investigation of oil-shale pyrolysis processing conditions using thermogravimetric analysis. Applied Energy, 66: 113-133.
Zhang, J., Ding, Y., Du, W., Lu, K., Sun, L., 2021. Study on pyrolyis kinetics and reaction mechanism of Beizao oil shale. Fuel, 296: 1-8.